Inorganic Chemistry

ARTICLE

pubs.acs.org/IC

Reductive Approach to Mixed Valency ($n = 1-$) in the Pyrazine Ligand-Bridged $[(acac)_2Ru(\mu\text{-}L^{2-})Ru(acac)_2]^n$ (L^{2-} = 2,5-Pyrazine-dicarboxylate) through Experiment and Theory

Amit Das,[†] Thomas Scherer,[‡] Somnath Maji,[†] Tapan Kumar Mondal,[§] Shaikh M. Mobin,[†] Francisco A. Urbanos,[∥,⊥] Reyes Jiménez-Aparicio,[*,∥] Wolfgang Kaim,[*,‡] and Goutam Kumar Lahiri[*,†]

[†]Department of Chemistry, Indian Institute of Technology Bombay, Powai, Mumbai-400076, India

[‡]Institut für Anorganische Chemie, Universität Stuttgart, Pfaffenwaldring 55, D-70550 Stuttgart, Germany

[§]Department of Chemistry, Jadavpur University, Jadavpur, Kolkata-700032, India

[∥]Departamento de Química Inorgánica, Facultad de Ciencias Químicas, Universidad Complutense, Ciudad Universitaria, E-28040 Madrid, Spain

Supporting Information

ABSTRACT: The diruthenium(III) complex $[(acac)_2Ru(\mu\text{-}L^{2-})Ru(acac)_2]$ (**1**) with $acac^-$ = acetylacetonato = 2,4-pentanedionato and a 2,5-pyrazine-dicarboxylato bridge, L^{2-}, has been obtained and structurally characterized as the *rac* ($\Delta\Delta$,$\Lambda\Lambda$) diastereomer. The $Ru^{III}Ru^{III}$ configuration in **1** (d_{Ru-Ru} = 6.799 Å) results in a triplet ground state (μ = 2.82 μ_B at 300 K) with a density functional theory (DFT) calculated triplet-singlet gap of 10840 cm^{-1} and the metal ions as the primary spin-bearing centers (Mulliken spin densities: Ru, 1.711; L, 0.105; acac, 0.184). The paramagnetic **1** exhibits broad, upfield shifted ^1H NMR signals with δ values ranging from −10 to −65 ppm and an anisotropic electron paramagnetic resonance (EPR) spectrum ($\langle g \rangle$ = 2.133, $g_1 - g_3 = \Delta g$ = 0.512), accompanied by a weak half-field signal at g = 4.420 in glassy frozen acetonitrile at 4 K. Compound **1** displays two closely spaced oxidation steps to yield labile cations. In contrast, two well separated reversible reduction steps of **1** signify appreciable electrochemical metal−metal interaction in the $Ru^{II}Ru^{III}$ mixed-valent state $\mathbf{1}^-$ ($K_c \approx 10^7$). The intermediate $\mathbf{1}^-$ shows a weak, broad $Ru^{II} \rightarrow Ru^{III}$ intervalence charge transfer (IVCT) band at about 1040 nm (ε = 380 M^{-1} cm^{-1}); the DFT approach for $\mathbf{1}^-$ yielded Mulliken spin densities of 0.460 and 0.685 for the two metal centers. The monitoring of the $\nu_{C=O}$ frequencies of the uncoordinated C=O groups of L^{2-} in $\mathbf{1}^n$ by IR spectroelectrochemistry suggests valence averaging ($Ru^{2.5}Ru^{2.5}$) in $\mathbf{1}^-$ on the vibrational time scale. The mixed-valent $\mathbf{1}^-$ displays a rhombic EPR signal ($\langle g \rangle$ = 2.239 and Δg = 0.32) which reveals non-negligible contributions from the bridging ligand, reflecting a partial hole-transfer mechanism and being confirmed by the DFT-calculated spin distribution (Mulliken spin density of −0.241 for L in $\mathbf{1}^-$). The major low energy electronic transitions in $\mathbf{1}^n$ (n = 0,−,2−) have been assigned as charge transfer processes with the support of TD-DFT analysis.

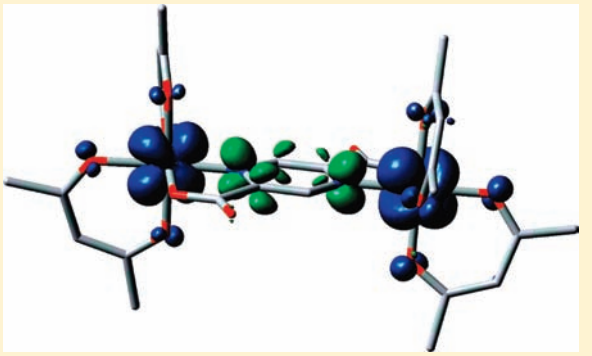

INTRODUCTION

The recognition of pyrazine-mediated intramolecular electron transfer in the mixed-valent $Ru^{II}(d^6)$-$Ru^{III}(d^5)$ states of the Creutz−Taube ion (**A**)[1] and of its cyano analogue (**B**)[2] has initiated several investigations using modified pyrazine-derived bridging ligands to understand the fundamentals related to intramolecular electron transfer.[3] Increased understanding of such electron transfer processes[3s,t,6] because of considerable theoretical,[4] methodological,[5] and conceptual advances over the past decades[6] has suggested a potential for applications of mixed-valent species in information transfer,[7] energy-relevant research,[8a,b] and optical devices.[8a]

The Creutz−Taube ion is the mixed-valent intermediate of a metal-centered two-step redox series involving $Ru^{II}Ru^{II}$, $Ru^{III}Ru^{II}$, and $Ru^{III}Ru^{III}$ states. Accompanying an enormous body of

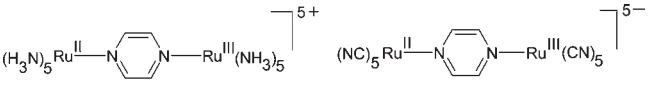

A **B**

experimental and theoretical work on the electronic structure and proper valence state description of the Creutz−Taube ion[6a−e] there were also several attempts to devise and study analogues with pyrazine-containing bridges,[7e,9] mostly starting from the typically better accessible $Ru^{II}Ru^{II}$ homovalent form.

In earlier work, the pyrazine-derived bis-chelating bridging ligand 2,5-pyrazine-dicarboxylate (L^{2-}), which offers the rare

Received: March 15, 2011
Published: June 29, 2011

combination[10] of both π acceptor (pyrazine) and donor (carboxylate) components as coordination centers, has been studied with respect to electrochemistry and spectroscopy of diruthenium complexes.[11] Ancillary ligands such as π-accepting 2,2′-bipyridine (bpy) in $[(bpy)_2Ru(\mu\text{-}L^{2-})Ru(bpy)_2]^{3+}$ (**C**), σ-donating NH_3 in $[(NH_3)_5Ru(\mu\text{-}L^{2-})Ru(NH_3)_5]^{3+}$(**D**), and unsymmetrical bpy/NH_3 in $[(NH_3)_5Ru(\mu\text{-}L^{2-})Ru(bpy)_2]^{3+}$ (**E**) were employed.[11] The mixed-valent states in symmetrical **C** and **D** were reported to exhibit moderate electrochemical interaction with comproportionation constants (K_c) of 10^3 and 10^5, respectively. The mixed-valent form **C** failed to show the expected intervalence charge transfer (IVCT) absorption from reduced Ru^{II} to oxidized Ru^{III} in the low-energy (near-infrared, NIR) region, while **D** and **E** exhibit weak IVCT bands.[11]

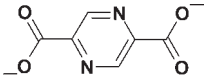

L^{2-}

The present article originates from our interest to investigate the effects from the electron-rich ancillary chelate ligand acetylacetonate ($acac^-$) on the intermetallic valence and spin−spin-interactions in the accessible redox states of $[(acac)_2Ru(\mu\text{-}L^{2-})Ru(acac)_2]^n$ (**1**^{n}). Unlike neutral

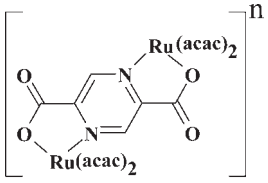

1^n

π-acceptor (bpy) or σ-donor (NH_3) ancillary ligands, the anionic $acac^-$ strongly stabilizes the ruthenium(III) (d^5, t_{2g}^5) state which extends the scope of investigations to magnetic interactions[12,13] between the Ru^{III} ions in the native state **1**, in addition to the study of electronic coupling in accessible mixed-valent intermediates.[12,13] Herein we present the synthesis, structural characterization, electrochemical behavior, and magnetic aspects of the isovalent $[(acac)_2Ru^{III}(\mu\text{-}L^{2-})Ru^{III}(acac)_2]$ (**1**). Most importantly, we describe in detail the very uncommon occurrence of strong ferromagnetic coupling through an extended molecular bridge. The mixed-valent state of $\{Ru^{III}(\mu\text{-}L^{2-})Ru^{II}\}$ in $\mathbf{1}^-$ has been scrutinized by UV−vis−NIR−IR spectroelectrochemistry and electron paramagnetic resonance (EPR) investigations in combination with density functional theory (DFT) calculations which were also performed for two-electron reduced $\mathbf{1}^{2-}$.

RESULTS AND DISCUSSION

The neutral complex $[(acac)_2Ru(\mu\text{-}L^{2-})Ru(acac)_2]$ (**1**) has been prepared and isolated in single isomer form from the precursor $[Ru(acac)_2(CH_3CN)_2]$ and 2,5-pyrazine-dicarboxylic acid (H_2L) under aerobic (oxidizing) conditions in the presence of NEt_3 as a base (see Experimental Section). The electron donating effects of the anionic terminal ($acac^-$) and bridging (L^{2-}) ligands favor the $(Ru^{III})_2$ state in **1**, as similarly observed for other $\{Ru(acac)_2\}$ containing complexes,[14] but in contrast to analogues with NH_3 or bpy coligands.[11,14] The low ruthenium(II/III) potential of −0.59 V versus SCE (see Table 3) confirms the facile metal oxidation under aerobic reaction conditions.

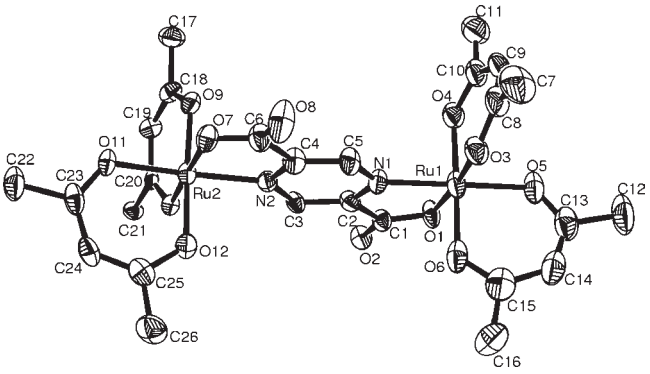

Figure 1. ORTEP diagram of **1** in the crystal of **1**x2 toluene. Ellipsoids are drawn at 50% probability level. Hydrogen atoms and solvents of crystallization are omitted for clarity.

Table 1. Selected Crystallographic Parameters of 1x2 Toluene

mol formula[a]	$C_{40}H_{30}N_2O_{12}Ru_2$
Fw	932.80
cryst sym	monoclinic
space group	*C*2/*c*
a/Å	30.95(3)
b/Å	20.23(19)
c/Å	14.13(15)
α/deg	90.0
β/deg	107.2(11)
γ/deg	90.0
V/Å^3	8448.8(15)
Z	8
μ/mm^{-1}	0.775
T/K	120(2)
D_{calcd}/g cm^{-3}	1.467
F/000	3744
θ range/deg	2.92 to 25.00
data/restraints/parameters	7366/0/443
R1, wR2 [$I > 2\sigma(I)$]	0.0609, 0.1490
R1, wR(all data)	0.1186, 0.1628
GOF	0.930
largest diff. peak/hole/e Å^{-3}	1.193, −0.512

[a] Molecule **1** and carbon atoms from two disordered toluene entities.

Compound **1** gives satisfactory microanalytical data (see Experimental Section) and exhibits a molecular ion peak, *m*/*z* at 766.13 in CH_3CN (Supporting Information, Figure S1), corresponding to **1** (calculated mass: 765.98). The molecular identity of **1** has been further authenticated by single-crystal X-ray structure analysis (Figure 1, Tables 1 and 2). Dinuclear tris-chelate complexes such as **1** can exist as pairs of enantiomers, *rac* (ΔΔ, ΛΛ; C_2 symmetry), or as the *meso* form (ΔΛ; C_s symmetry).[15,16] In the present case, the *rac* isomer has been isolated exclusively, as confirmed by its crystal structure and by preparative workup.

Each ruthenium(III) ion in **1** is bonded to the bridging L^{2-} through N(pyrazine) and O^- (carboxylate) donors to form a five-membered chelate ring. The bond angles around the ruthenium centers (Supporting Information, Table S1) reveal slightly

dx.doi.org/10.1021/ic200530u |*Inorg. Chem.* 2011, 50, 7040–7049

Table 2. Experimental and DFT Calculated Selected Bond Distances d/Å of 1 in the Crystal of 1x2 Toluene

bond length	exp.	calc.
Ru(1)−O(6)	1.972(6)	2.018
Ru(1)−O(3)	1.976(5)	2.0459
Ru(1)−O(4)	1.991(6)	2.040
Ru(1)−N(1)	2.002(6)	2.054
Ru(1)−O(1)	2.006(5)	2.026
Ru(1)−O(5)	2.029(5)	2.051
Ru(2)−O(12)	1.975(5)	2.019
Ru(2)−O(9)	1.988(5)	2.041
Ru(2)−O(10)	1.993(5)	2.043
Ru(2)−O(11)	2.021(5)	2.048
Ru(2)−O(7)	2.024(5)	2.026
Ru(2)−N(2)	2.034(6)	2.056
O(1)−C(1)	1.309(8)	1.310
O(2)−C(1)	1.221(8)	1.220
O(7)−C(6)	1.309(9)	1.310
O(8)−C(6)	1.210(9)	1.220
N(1)−C(2)	1.348(9)	1.351
N(1)−C(5)	1.358(9)	1.342
N(2)−C(3)	1.339(8)	1.342
N(2)−C(4)	1.346(9)	1.352
C(1)−C(2)	1.493(10)	1.516
C(2)−C(3)	1.402(9)	1.389
C(4)−C(5)	1.373(10)	1.389
C(4)−C(6)	1.505(10)	1.516

distorted octahedral arrangements. At 2.006(5) and 2.024(5) Å the Ru1−O1 and Ru2−O7 distances involving the L^{2-} bridge are slightly longer than the average Ru−O bond distance associated with the $acac^-$ groups of 1.993(5) Å. The Ru−O(acac) distances *trans* to Ru−N (L^{2-}) are about 0.03 Å longer than the other Ru−O(acac) distances because of the *trans* influence of the π-accepting pyrazine ring (Table 2). The Ru−O(acac) distances in **1** correspond to those of other structurally characterized $\{Ru(acac)_2\}$ complexes.[12,14,15b,24,26,31,34,38] The average Ru^{III}−O(L^{2-}) and Ru^{III}−N(L^{2-}) distances in **1** of 2.015(5) and 2.018(6) Å, respectively, are appreciably shorter than those reported for the diruthenium(II)-L^{2-} complex, $[\{(\eta^6\text{-}p\text{-}Pr^iC_6H_4Me)Ru^{II}Cl\}_2(\mu\text{-}L^{2-})]$, with 2.091(9) and 2.098(8) Å, respectively.[17] The average Ru^{III}−N(pyrazine, L^{2-}) distance of 2.018(6) Å in **1** is comparable to Ru−N(pyrazine) bond lengths of 2.020(13) and 2.049(12) Å, as observed for mixed-valent $[(cyclen)_4Ru_4(pz)_4]^{9+}$ (cyclen = 1,4,7,10-tetraazacyclododecane).[18] However, because of weaker Ru^{III} → pyrazine(L^{2-}) π-back-bonding interaction, that average Ru^{III}−N(pyrazine, L^{2-}) distance in **1** is longer than the corresponding value reported for the $(Ru^{2.5})_2$ Creutz−Taube ion (1.972(4)−2.002(2) Å)[3t] as well as for $[(A)Ru^{II}(\mu\text{-tppz})Ru^{II}(A)]^n$ (tppz = 2,3,5,6-tetrakis(2-pyridyl)pyrazine): A = bpy/Cl, 1.949(3) Å (bpy = 2,2′-bipyridine);[19] A = pap/Cl, 1.952(10) Å (pap = 2-phenylpyridine);[20] A = picolinate/Cl, 1.924(2) Å;[21] A = Q/Cl, 1.936(7) Å (Q = 4,6-di-*tert*.-butyl-*N*-phenyl-*o*-iminobenzosemiquinonato),[22] and in $(^tBuN)[Cl_3Ru^{II}(\mu\text{-tppz})Ru^{III}Cl_3]$, 1.912(4)/1.940(4) Å.[23]

The Ru−Ru distance in **1** is 6.799 Å, and the Ru^{III} ions are approximately coplanar with the pyrazine ring of L^{2-}. The calculated bond parameters of the DFT optimized **1** in the triplet ground state (Supporting Information, Figure S2) match well with the experimental data (Table 2 and Supporting Information, Table S1).

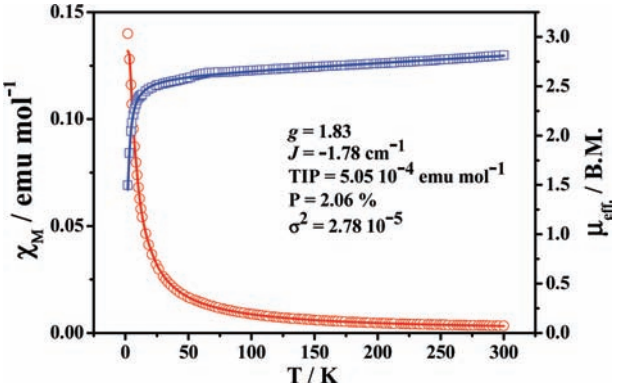

Figure 2. Temperature dependence of the magnetic susceptibility (circles) and the magnetic moment (squares) for **1**. Solid lines represents the fits obtained using the model explained in the text.

Magnetization measurements of **1** varying the magnetic field at 2 and 300 K for **1** do not show hysteresis loops (Supporting Information, Figures S3, S4), indicating the absence of any significant ferromagnetic interactions.[24] The magnetization changes almost linearly with the magnetic field; a slight deviation from linearity is observed at very low temperatures. The magnetization values at 300 K are close to those predicted by the Brillouin function but are lower at 2 K which suggests the existence of antiferromagnetic interactions at low temperatures. The magnetic susceptibility of **1** increases with decreasing temperature whereas the magnetic moment is not constant and decreases with temperature (Figure 2), confirming antiferromagnetic exchange coupling.

The magnetic moment of 2.82 μ_B at 300 K for **1** agrees well with the expected value for an $S = 1$ system, suggesting an uncommon ferromagnetic alignment of the two unpaired electrons within the dinuclear molecule-bridged system. However, the slope of the magnetic moment curve with decreasing temperature can be reproduced considering antiferromagnetic interactions between different *neighboring* molecules. The shortest *inter*molecular contact in the unit cell of **1** for through-space interaction was found at 5.688 Å between two spin-bearing ruthenium(III) centers (Figure 3) which is shorter than the *intra*molecular metal−metal distance of 6.799 Å, the metals being connected by an unsaturated bridge.

The magnetic moment curve at variable temperatures can be satisfactorily reproduced using the Bleaney−Bowers equation[25] for the contact between two $S = 1$ systems. The original formula needs to be multiplied by a factor of $^1/_2$ to calculate the magnetic susceptibility due to each dimetallic molecule. In addition, a TIP term and the presence of a paramagnetic impurity have been considered in eq 1.

$$\chi_M' = \frac{1}{2}\frac{Ng^2\beta^2}{kT} \times \frac{2e^{J/kT} + 10e^{3J/kT}}{1 + 3e^{J/kT} + 5e^{3J/kT}} + \text{TIP}$$

$$\chi_M = P\frac{2Ng^2\beta^2}{3kT} + (1 - P)\chi_M' \qquad (1)$$

The fit of the experimental data using this model leads to reasonable parameters ($g = 1.83$, $J = -1.78$ cm^{-1}, TIP = 5.05 × 10^{-4} emu mol^{-1}, and $P = 2.06\%$) with a good agreement

dx.doi.org/10.1021/ic200530u |*Inorg. Chem.* 2011, 50, 7040–7049

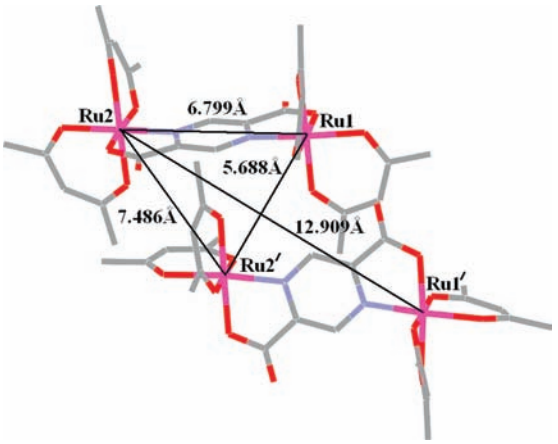

Figure 3. Ru−Ru distances in the unit cell of **1**x2 toluene.

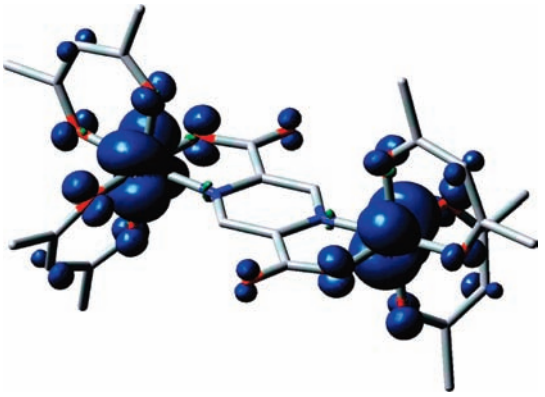

Figure 4. DFT calculated spin density representation of **1**.

between the experimental and calculated data (σ^2 = 2.78 × 10^{-5}), as can be seen in Figure 2.

The $Ru^{III}Ru^{III}$ configuration in **1** has been calculated with the triplet (S = 1) ground state 1.344 eV (10840 cm^{-1}) lower in energy than the corresponding spin-coupled singlet state (S = 0). The spin-density plot (Figure 4) from the DFT optimized structure of **1** in the S = 1 state (Supporting Information, Figure S2) reveals that the spins are primarily localized at the $[Ru(acac)_2]^+$ moieties; the Mulliken spin densities on Ru1, Ru2, L, and acac are 0.835, 0.846, 0.112, and 0.206, respectively. In agreement with these results, compound **1** displays a Ru^{III}-type (low-spin d^5) EPR signal with g_1= 2.37, g_2= 2.13, g_3 = 1.86; Δg = 0.51; $\langle g \rangle$ = 2.133 ($\Delta g = g_1 - g_3$ and $\langle g \rangle = [1/3(g_1^2 + g_2^2 + g_3^2)]^{1/2}$),[26] complemented by a weak half-field signal at g = 4.420 as expected for a triplet ground state (Figure 5).[27]

Compound **1** exhibits an ^{1}H NMR spectrum in $CDCl_3$ with a wide range of chemical shifts ($\delta \approx -10$ to -65 ppm) due to paramagnetic contact interactions (Figure 6, see Experimental Section).[14a,15,28] Partially overlapping eight methyl and four CH proton resonances corresponding to four non-equivalent acac ligands are observed, in addition to two "aromatic" protons from L^{2-}, as expected for the *rac* diastereoisomer.

Compound **1** displays two close-lying quasi-reversible oxidation processes in CH_3CN/0.1 M Et_4NClO_4 at 1.17 and 1.30 V versus SCE (Figure 7). They are considered to involve successive $Ru^{III} \rightarrow Ru^{IV}$ processes, leading to the $Ru^{IV}Ru^{IV}$ state via a mixed-valent

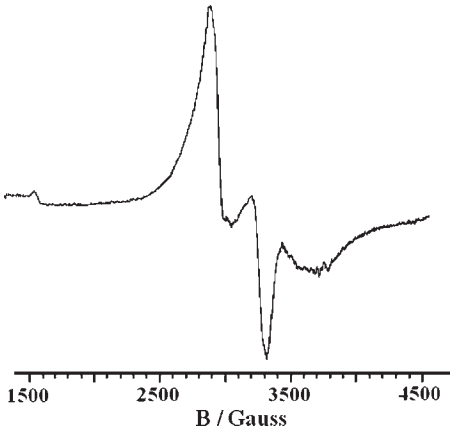

Figure 5. EPR spectrum of **1** in CH_3CN at 4 K.

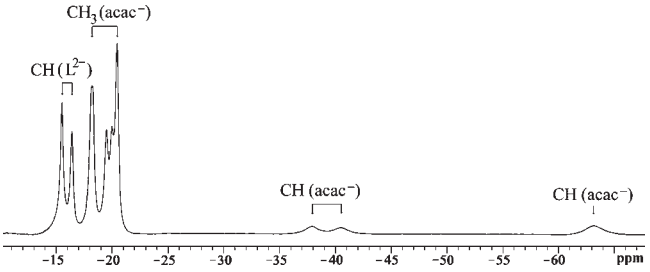

Figure 6. ^{1}H NMR spectrum of **1** in $CDCl_3$.

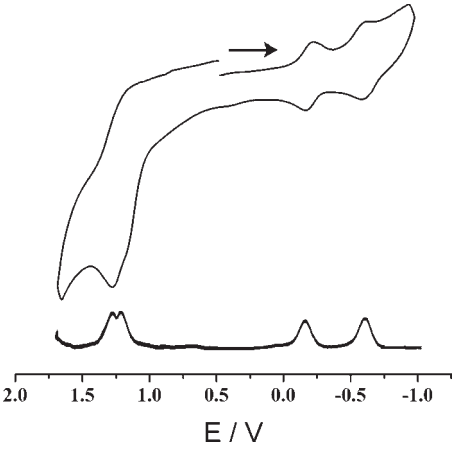

Figure 7. Cyclic and differential pulse voltammograms of **1**.

$Ru^{III}Ru^{IV}$ intermediate $\mathbf{1}^+$. The separation of 130 mV between the two oxidation processes as estimated by differential pulse voltammetry (Figure 7) would lead to a K_c value of 1.6 × 10^2 ($RT \ln K_c = nF\Delta E$)[29] (Figure 7), implying only weak electrochemical coupling. Higher K_c values for mixed-valent $Ru^{III}Ru^{IV}$ intermediates were reported for the related diruthenium-acac derivatives, $[(acac)_2Ru(\mu\text{-}1,4\text{-bis}(2\text{-phenolato})\text{-}1,4\text{-diazabutadiene})\text{-}Ru(acac)_2]$ (K_c = 1.7 × 10^6),[30] and $[(acac)_2Ru(\mu\text{-}2,5\text{-dioxido}\text{-}1,4\text{-benzoquinone})Ru(acac)_2]$ (K_c = $10^{7.8}$).[31] Spectroelectrochemistry (see below) confirms that the oxidation steps to $\mathbf{1}^+$ and $\mathbf{1}^{2+}$ are not completely reversible, limiting their further discussion.

dx.doi.org/10.1021/ic200530u |*Inorg. Chem.* 2011, 50, 7040–7049

Table 3. Redox Potentials and Comproportionation Constants

compounds (starting form)	$E_{298}°$/V[a] $Ru^{III}Ru^{III}/Ru^{III}Ru^{II}$	$Ru^{III}Ru^{II}/Ru^{II}Ru^{II}$	ΔE_p[b]/mV	K_{c1}[c,d]	ref.
$[(bpy)_2Ru(\mu\text{-}L^{2-})Ru(bpy)_2]^{2+}$	1.40[e]	1.22[e]	180	1.1×10^3	11
$[(NH_3)_4Ru(\mu\text{-}L^{2-})Ru(NH_3)_4]^{2+}$	0.86[f]	0.56[f]	300	1.2×10^5	11
$[(NH_3)_4Ru(\mu\text{-}L^{2-})Ru(bpy)_2]^{2+}$	1.35[e]	0.55[e]	800	3.6×10^{13}	11
$[(acac)_2Ru(\mu\text{-}L^{2-})Ru(acac)_2]$ (**1**)	−0.17[g]	−0.59[g]	420	1.3×10^7	this work

[a] Potential in V versus SCE. [b] ΔE_p: Peak potential difference. [c] Comproportionation constant from $RT \ln K_c = nF(\Delta E)$. [d] K_{c1} between red 1 and red 2. [e] Cyclic voltammetry in CH_3CN/0.1 M $(t\text{-}Bu_4)NPF_6$. [f] Cyclic voltammetry in 0.001 M HCl/0.1 M KCl. [g] Cyclic voltammetry in CH_3CN/0.1 M Et_4NClO_4 at 100 mV s^{-1}.

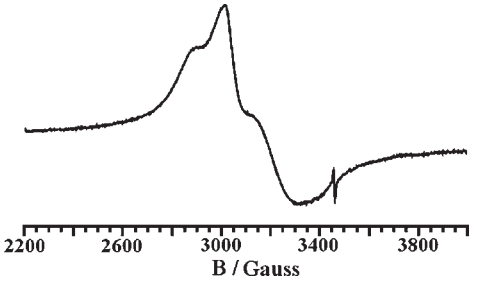

Figure 8. EPR spectrum of $\mathbf{1}^-$ in CH_3CN at 110 K.

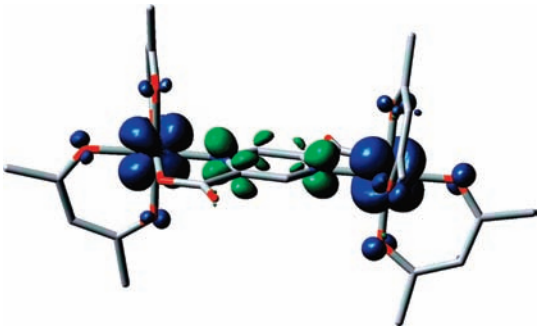

Figure 9. DFT calculated spin density plot of $\mathbf{1}^-$.

In contrast, the fully reversible reduction of one of the Ru^{III} centers in **1** to Ru^{II} in the mixed-valent $\{Ru^{III}(\mu\text{-pyrazine})Ru^{II}\}$ state of $\mathbf{1}^-$ results in much stronger intermetallic electrochemical coupling ($K_c \sim 10^7$) due to $t_{2g}^6(Ru^{II}) \rightarrow$ pyrazine(L^{2-}) π-back-bonding (see later).

After the initial successive two reductions of $Ru^{III}Ru^{III}$ in **1** to $Ru^{II}Ru^{II}$ in $\mathbf{1}^{2-}$ a further reduction involving the pyrazine ring of coordinated L^{2-} could be conceived.[32] However, no such reduction step has been detected within the experimental potential range down to −2.0 V versus SCE.

In comparison to the analogous symmetrical complexes with the neutral π-acidic bpy ancillary ligands in $[(bpy)_2Ru^{II}(\mu\text{-}L^{2-})\text{-}Ru^{II}(bpy)_2]^{2+}$ [11] or the σ-donating NH_3 ligands in $[(NH_3)_4\text{-}Ru^{II}(\mu\text{-}L^{2-})Ru^{II}(NH_3)_4]^{2+}$,[11] the Ru^{III}/Ru^{II} couples in **1** are significantly shifted to lower potentials by more than 1 V (Table 3) because of the difference in electronic properties of the ancillary ligands (bpy, NH_3, $acac^-$), as has similarly been documented earlier.[33] By virtue of more electron density on the Ru centers in **1** because of the electron donating effect of the negatively charged chelates $acac^-$, the system also exhibits stronger electrochemical coupling as reflected by the K_c values of 10^7 for **1** versus 10^3 and 10^5 for the bpy and NH_3 ligated derivatives **C** and **D**,[11] respectively.

The mixed-valent $\mathbf{1}^-$ displays an anisotropic EPR spectrum at 110 K with $g_1 = 2.400$, $g_2 = 2.229$, $g_3 = 2.076$, $\Delta g = 0.32$, and $\langle g \rangle = 2.239$ (Figure 8), corresponding to a Ru^{III} configuration.[34] However, the g anisotropy is smaller than that reported for the Creutz−Taube ion ($g_1 = 2.799$, $g_2 = 2.489$, $g_3 = 1.346$, $\Delta g = 1.453$, and $\langle g \rangle = 2.298$[35]) and also smaller than that of the triplet precursor **1** (see above) which implies more contribution from the radical bridge to the singly occupied MO in $\mathbf{1}^-$. This would be expected for a partial hole-transfer valence exchange mechanism[6d,g,36] involving a mixed donor/acceptor bridge such as 2,5-pyrazine-dicarboxylate. In the hole-transfer mechanism for metal−metal valence exchange the highest occupied molecular orbital (HOMO) of the electron-rich bridging ligand can facilitate this exchange by getting fractionally depopulated (partial ligand oxidation).[6d,g,36] The spin-density plot of $\mathbf{1}^-$ (Figure 9) from DFT calculations confirms this interpretation by showing Mulliken spin densities on Ru1, Ru2, L, and acac of 0.655, 0.357, −0.170, and 0.157, respectively. Unfortunately, the broad EPR signal of $\mathbf{1}^-$ has prevented attempts to determine the extent of (de)localization on the basis of $^{99,101}Ru$ hyperfine coupling.[37] The mixed-valent $Ru^{II}Ru^{III}$ state in $\mathbf{1}^-$ failed to show any EPR signal at 298 K, presumably because of rapid relaxation[38] favored by the high spin−orbit coupling constant of Ru^{III}.[39]

UV−vis−NIR absorption spectra were obtained for **1**, $\mathbf{1}^-$, and $\mathbf{1}^{2-}$, and were analyzed by time-dependent DFT (TD-DFT) calculations which allowed for tentative assignments. Calculated spectra (Supporting Information, Figures S8−S10) lend further confidence to these assignments.

In CH_3CN the neutral complex **1** exhibits one intense absorption band at 540 nm in addition to intense, mostly ligand-based absorptions in the UV-region which will not be further discussed (Figure 10, Table 4). The low energy absorption feature in the visible region can be assessed via TD-DFT calculations (Table 5, Supporting Information, Figure S8), based on the optimized structure of **1** (Supporting Information, Figure S2) in the triplet state; it involves several metal-to-ligand charge-transfer (MLCT) as well as ligand-to-metal charge transfer (LMCT) transitions.

The irreversible nature of the oxidation processes (Figure 7, Table 3) has precluded our attempts to investigate spectral changes after oxidation by spectroelectrochemistry. However, the reversible reduction behavior facilitated the electrochemical generation and spectroscopic characterization of the corresponding one-electron reduced mixed-valent $Ru^{III}Ru^{II}$ ($\mathbf{1}^-$) and of isovalent $Ru^{II}Ru^{II}$ ($\mathbf{1}^{2-}$) states. On one-electron reduction of **1** to $\mathbf{1}^-$ the

dx.doi.org/10.1021/ic200530u |*Inorg. Chem.* 2011, 50, 7040–7049

intensity of the lowest energy absorption at 540 nm (MLCT, see Tables 4) reduces from ε = 8100 M^{-1} cm^{-1} to 6300 M^{-1} cm^{-1}. A second MLCT ($Ru \rightarrow L^{2-}$) band is observed in agreement with the mixed-valent status at 625 nm (ε = 7530 M^{-1} cm^{-1}). Most characteristically, the mixed-valent $Ru^{II}Ru^{III}$ form in $\mathbf{1}^-$ displays one weak, broad near-IR absorption at about 1040 nm (ε = 380 M^{-1} cm^{-1}), corresponding to a $Ru^{II} \rightarrow Ru^{III}$ intervalence charge-transfer transition (IVCT).

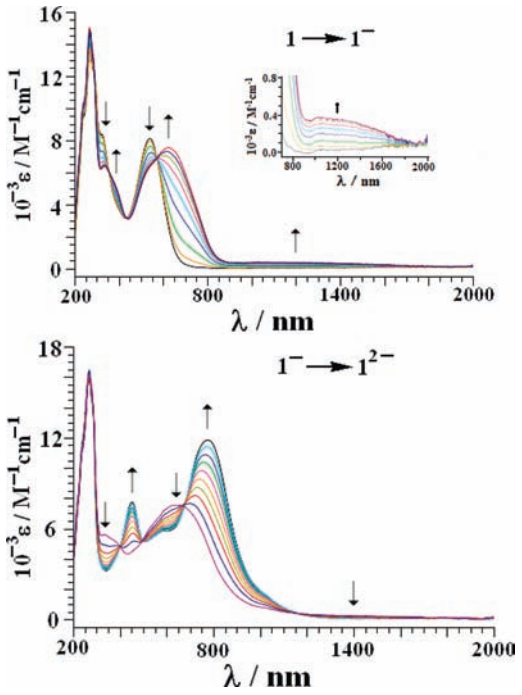

Figure 10. UV−vis−NIR spectroelectrochemistry for the conversions of (a) $\mathbf{1} \rightarrow \mathbf{1}^-$ and (b) $\mathbf{1}^- \rightarrow \mathbf{1}^{2-}$ in CH_3CN/0.1 M Bu_4NPF_6.

Table 4. UV/Vis/NIR Spectroelectrochemical Data for $\mathbf{1}^n$ in CH_3CN/0.1 M Bu_4NPF_6

compound	λ /nm (ε /M^{-1} cm^{-1})
1	540(8100), 330(8470), 275(15500)
$\mathbf{1}^-$	1040(380), 625(7530), 540(6400), 375sh, 330(6470), 275(13250)
$\mathbf{1}^{2-}$	775(11950), 590sh, 450(7850), 275(16530)

The TD-DFT calculations on the optimized structure of $\mathbf{1}^-$ in the doublet state (Table 6) also predict one low-energy band at 1300 nm involving a $Ru(d\pi) \rightarrow Ru(d\pi)$ transition. The calculations also predict two transitions at 613 and 553 nm, corresponding to $Ru(d\pi) \rightarrow L(\pi^*)$, that is, MLCT processes $SOMO(\alpha) \rightarrow LUMO(\alpha)$ and $HOMO-1(\alpha) \rightarrow LUMO(\alpha)$, respectively (Supporting Information, Figure S9).

The broadness of the IVCT absorption and its overlap with the tailing of the nearby intense band in the visible did not allow us to make an estimate of the bandwidth at half height ($\Delta\nu_{1/2}$) for the IVCT absorption. The Hush formalism[4] could thus not be applied. The broadness of the weak IVCT absorption and the splitting of the band around 600 nm seem to point to a localized mixed-valent $Ru^{II}Ru^{III}$ state in $\mathbf{1}^-$ on the electron spectroscopic time scale, even though the charge-dependent electrochemical coupling in the form of the K_c value of 10^7 seems to suggest a delocalized mixed-valent situation. It has been noted before, however, that bis-chelate diruthenium(III,II) systems display unusually low-intensity IVCT bands despite strong valence coupling;[6e,35b] the low charge of $\mathbf{1}^-$ makes it also less susceptible to charge trapping of localized valences.

To derive an additional understanding of the valence situation, that is, probing the localized versus delocalized alternative for mixed-valent $\mathbf{1}^-$, the change in the $\nu_{C=O}$ frequency of the uncoordinated carbonyl function of the carboxylate substituent in L^{2-} on successive electron transfer has been monitored by IR-spectroelectrochemistry. The shifts of metal carbonyl bands[3t,40] as well as of uncoordinated carbonyl groups of organic ligands such as chelating dipyridyl ketone[41] or 2,2′-bis(1-methylimidazolyl)-ketone[42] have been used recently to study the charge and (de)-localization situation in mixed-valent complexes. The $\nu_{C=O}$ frequency of the carboxylate functions of coordinated L^{2-} in the parent complex **1** with isovalent $\{Ru^{III}(\mu\text{-}L^{2-})Ru^{III}\}$ center appears at 1675 cm^{-1}. It shifts to lower-energies at 1641 cm^{-1} and 1626 cm^{-1} on successive one-electron reduction to $\{Ru^{III}(\mu\text{-}L^{2-})Ru^{II}\}$ ($\mathbf{1}^-$)

Table 5. TD-DFT Data for 1 in Triplet (S = 1) Ground State in CH_3CN

$E_{excitation}$ (eV)	$\lambda_{excitation}$ (nm)	osc. strength (f)	λ_{max} (expt.) (nm)	key transitions	character
2.130	582	0.040	540	(63%)HOMO-1(β)→LUMO+2(β)	$Ru^{III}(d\pi) \rightarrow L(\pi^*)$, MLCT
2.280	544	0.070	540	(61%)SOMO2(α)→LUMO(α)	$Ru^{III}(d\pi)$/acac(π)→$L(\pi^*)$, MLCT/ILCT
2.340	530	0.060	540	(38%)HOMO-6(β)→LUMO+1(β)	acac(π)→$Ru^{III}(d\pi)$, LMCT
				(37%)HOMO-7(β)→LUMO(β)	
2.510	493	0.100	540	(73%)HOMO-2(α)→LUMO(α)	$Ru^{III}(d\pi) \rightarrow L(\pi^*)$, MLCT
2.750	451	0.030		(41%)HOMO-9(β)→LUMO(β)	$L(\pi) \rightarrow Ru^{III}(d\pi)$, LMCT
				(31%)HOMO-8(β)→LUMO(β)	
3.140	395	0.030		(47%)HOMO-9(β)→LUMO+1(β)	$L(\pi)$/acac(π)→$Ru^{III}(d\pi)$, LMCT
				(22%)HOMO-10(β)→LUMO(β)	
3.640	340	0.060	330	(67%)HOMO-8(α)→LUMO(α)	$L(\pi) \rightarrow L(\pi^*)$, ILCT
4.110	302	0.070		(43%)HOMO-14(α)→LUMO(α)	$L(\pi)$/acac(π)→$L(\pi^*)$, ILCT
				(29%) HOMO-15(α)→LUMO(α)	
4.260	291	0.050		(53%) HOMO-8(β)→LUMO+2(β)	$L(\pi) \rightarrow L(\pi^*)$, ILCT
				(20%) HOMO-9(β)→LUMO+2(β)	
4.500	275	0.120	275	(53%) HOMO-9(β)→LUMO+3(β)	$L(\pi)$/acac(π)→$L(\pi^*)$, ILCT
				(20%) HOMO-10(β) →LUMO+2(β)	

dx.doi.org/10.1021/ic200530u |Inorg. Chem. 2011, 50, 7040–7049

Table 6. TD-DFT Data for 1^- in Doublet ($S = 1/2$) Ground State in CH_3CN

$E_{excitation}$ (eV)	$\lambda_{excitation}$ (nm)	osc. strength (f)	λ_{max} (expt.) (nm)	key transitions	character
0.950	1300	0.050	1040	(51%)HOMO-2(β)→LUMO(β)	$Ru^{II}(d\pi)(2)\rightarrow Ru^{III}(d\pi)(1)$, IVCT
				(32%)HOMO-1(β)→LUMO(β)	
2.020	613	0.070	625	(70%)SOMO(α)→LUMO(α)	$Ru^{II}(d\pi)(2)\rightarrow L(\pi^*)$, MLCT
2.240	553	0.050	540	(46%)HOMO-1(α)→LUMO(α)	$Ru^{II}(d\pi)(2)\rightarrow L(\pi^*)$, MLCT
2.880	431	0.010		(72%)HOMO-8(β)→LUMO(β)	$L(\pi)/acac(\pi)\rightarrow Ru^{III}(d\pi)(1)$, LMCT
3.020	410	0.020		(63%)HOMO-11(β) →LUMO(β)	$L(\pi)\rightarrow Ru^{III}(d\pi)$ (1), LMCT
3.250	382	0.040	375	(55%)HOMO-13(β)→LUMO(β)	$L(\pi)/acac(\pi)\rightarrow Ru^{III}(d\pi)(1)$, LMCT
				(23%)HOMO-14(β)→LUMO(β)	
3.740	331	0.050	330	(64%)HOMO-8(α)→LUMO(α)	$L(\pi)\rightarrow L(\pi^*)$, ILCT
3.960	313	0.050		(59%)HOMO-11(α)→LUMO(α)	$L(\pi)\rightarrow L(\pi^*)$, ILCT
4.170	297	0.040		(66%)HOMO-13(β)→LUMO+1(β)	$L(\pi)\rightarrow L(\pi^*)$, ILCT
4.370	284	0.090	275	(40%)HOMO-14(β)→LUMO+1(β)	$L(\pi)\rightarrow L(\pi^*)$, ILCT
				(33%)HOMO-14(β)→LUMO+2(β)	$L(\pi)\rightarrow acac(\pi^*)$, ILCT
4.650	266.4	0.110		(43%)HOMO-14(β)→LUMO+2(β)	$L(\pi)\rightarrow acac(\pi^*)$, ILCT
				(28%)HOMO-16(β)→LUMO+2(β)	

and $\{Ru^{II}(\mu\text{-}L^{2-})Ru^{II}\}$ ($\mathbf{1}^{2-}$) species, respectively (Figure 11). The shifting of the $\nu_{C=O}$ frequency without any distinct splitting for the EPR-established mixed-valent $\{Ru^{III}(\mu\text{-}L^{2-})Ru^{II}\}$ intermediate state in $\mathbf{1}^-$ appears to support a valence averaged formulation on the vibrational time scale, leading to a $Ru^{2.5}Ru^{2.5}$ situation as reflected also by the large K_c value of 10^7 and the almost even spin distribution calculated for both the ruthenium centers. The small broadening of the $\nu_{C=O}$ band for the mixed-valent intermediate in $\mathbf{1}^-$ ($\Delta\nu_{1/2}$: 30 cm^{-1}) with respect to the isovalent states of **1** ($Ru^{III}Ru^{III}$) ($\Delta\nu_{1/2}$: 20 cm^{-1}) and $\mathbf{1}^{2-}$ ($Ru^{II}Ru^{II}$) ($\Delta\nu_{1/2}$: 22 cm^{-1}) is not considered significant enough for warrant a partial class II mixed-valent formulation under the chosen experimental conditions.

On further one-electron reduction of the $Ru^{II}Ru^{III}$ state in $\mathbf{1}^-$ to the isovalent $Ru^{II}Ru^{II}$ form $\mathbf{1}^{2-}$, the IVCT band expectedly disappears and the close lying charge transfer bands in the visible fall into a single absorption band at 775 nm with an enhancement in intensity (ε = 11950 M^{-1} cm^{-1}) (Figure 10, Supporting Information, Figure S10 and Table 4). The TD-DFT calculations on the optimized singlet state of $\mathbf{1}^{2-}$ also predict one band at 765 nm involving MLCT ($Ru(d\pi)\rightarrow L(\pi^*)$) transitions corresponding to HOMO→LUMO/HOMO−2→LUMO (Table 7).

CONCLUSIONS

Taking advantage of the electron rich $[Ru(acac)_2]^n$ complex fragment with its propensity to get stabilized in the Ru^{III} (n = +) rather than the Ru^{II} (n = 0) oxidation state we have isolated a homovalent neutral $Ru^{III}Ru^{III}$ species **1** with the carboxylate functionalized pyrazine bridging ligand 2,5-pyrazine-dicarboxylate and identified it as the *rac*-isomer in the triplet ground state through X-ray diffraction, spectroscopic, and magnetic studies. We could describe in detail the very uncommon occurrence of strong ferromagnetic coupling through an extended molecular bridge. Stepwise reduction monitored by spectroelectrochemistry produced a monoanionic mixed-valent intermediate, characterized by a broad, long-wavelength intervalence charge transfer (IVCT) band at about 1040 nm, a rhombic EPR signal reflecting partial spin accommodation by the bridge, and an unsplit ν(CO) vibrational band from the bridging ligand in the IR experiment. While the weak IVCT absorption (ε = 380 M^{-1} cm^{-1}) may

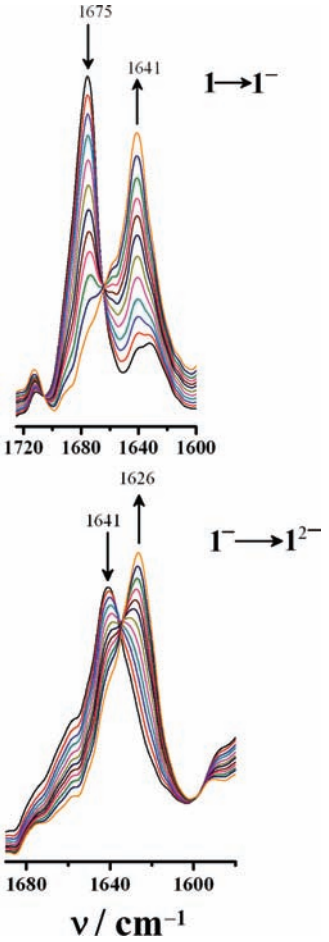

Figure 11. IR-spectroelectrochemistry for the conversions of **1**→ $\mathbf{1}^-$ and $\mathbf{1}^-$→ $\mathbf{1}^{2-}$ in CH_3CN/0.1 M Bu_4NPF_6.

suggest limited electronic coupling, the IR result and the large comproportionation constant of $K_c = 10^7$ point to delocalized valence on the vibrational time scale, according to a $Ru^{2.5}Ru^{2.5}$ formulation or, at least, to a borderline situation.[6e] Low intensity IVCT absorptions are not uncommon for strongly coupled

dx.doi.org/10.1021/ic200530u |*Inorg. Chem.* 2011, 50, 7040–7049

Table 7. TD-DFT Data for 1^{2-} in Singlet ($S = 0$) Ground State in CH_3CN

$E_{excitation}$ (eV)	$\lambda_{excitation}$ (nm)	osc. strength (f)	λ_{max} (expt.) (nm)	key transitions	character
1.620	765	0.110	775	(68%)HOMO→LUMO	$Ru^{II}(d\pi)$→$L(\pi^*)$, MLCT
				(26%)HOMO-2→LUMO	
2.150	577	0.060	590	(50%)HOMO-2→LUMO	$Ru^{II}(d\pi)$→$L(\pi^*)$, MLCT
				(23%)HOMO→LUMO	
2.600	477	0.040		(67%)HOMO-1→LUMO+1	$Ru^{II}(d\pi)$→acac(π^*), MLCT
2.700	460	0.070	450	(69%)HOMO-2→LUMO+1	$Ru^{II}(d\pi)$→acac(π^*), MLCT
2.850	435	0.030		(78%)HOMO-4→LUMO+1	$Ru^{II}(d\pi)$→acac(π^*), MLCT
3.130	396	0.030		(46%)HOMO-1→LUMO+4	$Ru^{II}(d\pi)$→acac(π^*), MLCT
				(26%)HOMO→LUMO+5	$Ru^{II}(d\pi)$→$L(\pi^*)$, MLCT
3.910	317	0.040		(43%)HOMO-6→LUMO+5	$L(\pi)$→$L(\pi^*)$, ILCT
				(27%)HOMO-7→LUMO+4	$L(\pi)$/acac(π)→acac(π^*), ILCT
4.250	292	0.050		(50%)HOMO-9→LUMO+2	$L(\pi)$/acac(π)→acac(π^*), ILCT
				(23%)HOMO-8→LUMO+2	
4.380	283	0.110	275	(67%)HOMO-17→LUMO	$L(\pi)$→ $L(\pi^*)$, ILCT
4.600	270	0.130		(39%)HOMO-22→LUMO	$L(\pi)$→ $L(\pi^*)$, ILCT
				(29%)HOMO-23→LUMO	

bis-chelate systems,[6f,35b] but have been analyzed here for the first time for a mixed donor/acceptor bridged example by use of electronic, vibrational, and EPR spectroelectrochemical techniques in conjunction with DFT calculations. The redox series $\mathbf{1}^{n-}$ also illustrates how low-charged diruthenium(III,II) species (with less propensity for valence and charge trapping) can be accessible via reduction from paramagnetic $Ru^{III}Ru^{III}$ precursors instead of the conventional oxidative generation. Stabilization of the electrochemically accessible cation and dication for experimental studies will require synthetic modifications which will be attempted in future work.

EXPERIMENTAL SECTION

Materials. The starting complex $[Ru(acac)_2(CH_3CN)_2]$ was prepared according to the reported procedure.[43] The ligand 2,5-pyrazine dicarboxylic acid was purchased from Aldrich. Other chemicals and solvents were of reagent grade and used as received. For spectroscopic and electrochemical studies HPLC grade solvents were used. Commercial tetraethylammonium bromide was converted into pure tetraethylammonium perchlorate following a published procedure.[44]

Physical Measurements. UV−vis−NIR and IR spectroelectrochemical studies were performed in CH_3CN/0.1 M Bu_4NPF_6 at 298 K using an optically transparent thin layer electrode (OTTLE) cell mounted in the sample compartments of a J&M Tidas spectrophotometer or a Perkin-Elmer 1760X FTIR instrument, respectively.[45] ^1H NMR spectrum was obtained with a 300 MHz Varian FT spectrometer. The EPR measurements were made in a two-electrode capillary tube[46] with an X-band Bruker system ESP300, equipped with a Bruker ER035 M gaussmeter and a HP 5350B microwave counter. Cyclic voltammetric, differential pulse voltammetric, and coulometric measurements were performed using a PAR model 273A electrochemistry system with platinum wire working and auxiliary electrodes and an aqueous saturated calomel reference electrode (SCE) in a three-electrode configuration. The supporting electrolyte was Et_4NClO_4, and the solute concentration was $\sim 10^{-3}$ M. The half-wave potential E°_{298} was set equal to $0.5(E_{pa} + E_{pc})$, where E_{pa} and E_{pc} are anodic and cathodic cyclic voltammetric peak potentials, respectively. Elemental analysis was carried out with a Perkin-Elmer 240C elemental analyzer. Electrospray mass spectrum was recorded on a Micromass Q-ToF mass spectrometer.

Preparation of $[(acac)_2Ru^{III}(\mu\text{-}L)Ru^{III}(acac)_2]$. Excess NEt_3 (0.1 mL, 0.8 mmol) was added to a 5 mL ethanolic solution of the ligand, 2,5-pyrazine-dicarboxylic acid (22 mg, 0.13 mmol). This was then added dropwise to a 30 mL ethanolic solution of $[Ru(acac)_2(CH_3CN)_2]$ (100 mg, 0.26 mmol). The mixture was heated to reflux for 8 h under atmospheric conditions. The initial orange solution gradually changed to violet. The solvent was evaporated to dryness under reduced pressure, and the solid mass thus obtained was purified by using a silica gel column. Initially a red band of $[Ru(acac)_3]$ was eluted with CH_2Cl_2. Further elution by CH_3CN gave a bright violet band corresponding to the complex **1** which was isolated by solvent evaporation. Yield, 58 mg (60%). Anal. Calcd. for $C_{26}H_{30}N_2O_{12}Ru_2$: C, 40.73; H, 3.95; N, 3.66. Found: C, 40.75; H, 3.87; N, 3.54. ESI MS (in CH_3CN): $m/z = 766.13$ corresponding to $[\mathbf{1}]^+$ (calcd. molecular weight: 765.99). ^1H NMR in $CDCl_3$ (δ, ppm): CH(L^{2-}): −15.51, −16.40; CH_3(acac): −18.20, −19.49, −19.98, −20.42; CH(acac): −37.89, −40.56, −63.17. IR(KBr disk): ν(C═O), 1671 cm^{-1}.

Crystal Structure Determination. Single crystals were grown by slow evaporation of a 1:1 acetonitrile-toluene solution of **1**. The crystal data were collected on an Oxford X-CALIBUR-S CCD diffractometer at 120 K. Selected data collection parameters and other crystallographic results are summarized in Table 1. All data were corrected for Lorentz polarization and absorption effects. The program package of SHELX-97[47] was used for structure solution and full matrix least-squares refinement on F^2. Hydrogen atoms were included in the refinement using the riding model. The hydrogen atoms associated with the disordered toluene molecules could not be located. The disordered toluene molecules were refined isotropically.

Magnetic Measurements. The variable-temperature magnetic susceptibilities were measured on polycrystalline samples with a Quantum Design MPMS*XL* SQUID (Superconducting Quantum Interference Device) susceptometer over a temperature range of 2 to 300 K at the constant field of 1 T. Each raw data set was corrected for the diamagnetic contribution of both the sample holder and the complex to the susceptibility. The molar diamagnetic corrections were calculated on the basis of Pascal constants. Magnetization measurements were carried out at 2 and 300 K from 0 to 5 T including also cycles between −5 and 5 T to check the existence of hysteresis loops. The fitting of the experimental data was carried out using the MATLAB V.6.5.0.180913a program.

Computational Details. Full geometry optimizations were carried out using the DFT method at the (U)B3LYP level for **1** and $\mathbf{1}^-$ and (R)-B3LYP for $\mathbf{1}^{2-}$.[48] All elements except ruthenium were assigned the 6-31G(d) basis set. The SDD basis set with effective core potential was

dx.doi.org/10.1021/ic200530u |*Inorg. Chem.* 2011, 50, 7040–7049

employed for the ruthenium atom.[49] The vibrational frequency calculations were performed to ensure that the optimized geometries represent the local minima and there are only positive eigenvalues. All calculations were performed with Gaussian03 program package.[50] Vertical electronic excitations based on (U)B3LYP/(R)B3LYP optimized geometries were computed for **1**, $\mathbf{1}^{-}$, and $\mathbf{1}^{2-}$ using the TD-DFT formalism[51] in acetonitrile using the conductor-like polarizable continuum model (CPCM).[52] GaussSum[53] was used to calculate the fractional contributions of various groups to each molecular orbital.

■ ASSOCIATED CONTENT

Supporting Information. X-ray crystallographic file in CIF format, mass spectrum, DFT calculated optimized structure, magnetization curves of **1**, DFT calculated MO pictures of **1**, $\mathbf{1}^{-}$, $\mathbf{1}^{2-}$, experimental and theoretical spectra of **1**, $\mathbf{1}^{-}$, $\mathbf{1}^{2-}$ (Figures S1−S10), experimental and DFT calculated bond angles of **1** and DFT calculated MO compositions of **1**, $\mathbf{1}^{-}$, $\mathbf{1}^{2-}$ (Tables S1−S4). This material is available free of charge via the Internet at http://pubs.acs.org.

■ AUTHOR INFORMATION

Corresponding Author

*E-mail: kaim@iac.uni-stuttgart.de (W.K.), lahiri@chem.iitb.ac.in (G.K.L.).

Notes

⊥Deceased, May 28, 2011.

■ ACKNOWLEDGMENT

Financial support received from the Department of Science and Technology and the Council of Scientific and Industrial Research (fellowship to A.D.), New Delhi (India), the DAAD, FCI, and DFG (Germany), the Spanish MICINN, CM, and UCM-BSCH (projects nos. CTQ2008-00920, S2009/MAT-1467, and UCM-921073-4120824), is gratefully acknowledged. X-ray structural study for **1** was carried out at the National Single Crystal Diffractometer Facility, Indian Institute of Technology, Bombay. Special acknowledgment is made to the Sophisticated Analytical Instrument Facility (SAIF), Indian Institute of Technology, Bombay, for providing the NMR facility.

■ REFERENCES

(1) (a) Creutz, C.; Taube, H. *J. Am. Chem. Soc.* **1969**, *91*, 3988. (b) Creutz, C.; Taube, H. *J. Am. Chem. Soc.* **1973**, *95*, 1086.

(2) Scheiring, T.; Kaim, W.; Olabe, J. A.; Parise, A. R.; Fiedler, J. *Inorg. Chim. Acta* **2000**, *125*, 300.

(3) (a) Rillema, D. P.; Mack, K. B. *Inorg. Chem.* **1982**, *21*, 3849. (b) Braunstein, C. H.; Baker, A. D.; Strekas, T. C.; Gafney, H. D. *Inorg. Chem.* **1984**, *23*, 857. (c) Ruminski, R. R.; Cockroft, T.; Shoup, M. *Inorg. Chem.* **1988**, *27*, 4026. (d) Balzani, V.; Juris, A.; Venturi, M.; Campagna, S.; Serroni, S. *Chem. Rev.* **1996**, *96*, 759. (e) Gourdon, A.; Launay, J.-P. *Inorg. Chem.* **1998**, *37*, 5336. (f) Bonhote, P.; Lecas, A.; Amouyal, E. *Chem. Commun.* **1998**, 885. (g) Denti, G.; Campagna, S.; Sabatino, L.; Serroni, S.; Ciano, M.; Balzani, V. *Inorg. Chem.* **1990**, *29*, 4750. (h) Stadler, A.-M.; Puntoriero, F.; Campagna, S.; Kyritsakas, N.; Welter, R.; Lehn, J.-M. *Chem.—Eur. J.* **2005**, *11*, 3997. (i) Browne, W. R.; O'Boyle, N. M.; Henry, W.; Guckian, A. L.; Horn, S.; Fett, T.; O'Connor, C. M.; Duati, M.; Cola, L. D.; Coates, C. G.; Ronayne, K. L.; McGarvey, J. J.; Vos, J. G. *J. Am. Chem. Soc.* **2005**, *127*, 1229. (j) D'Alessandro, D. M.; Topley, A. C.; Davies, M. S.; Keene, F. R. *Chem.—Eur. J.* **2006**, *12*, 4873. (k) D'Alessandro, D. M.; Keene, F. R. *New J. Chem.* **2006**, *30*, 228. (l) Maji, S.; Sarkar, B.; Mobin, S. M.; Fiedler, J.; Kaim, W.; Lahiri, G. K. *Dalton Trans.* **2007**, 2411. (m) Loiseau, F.; Nastasi, F.; Stadler, A.-M.; Campagna, S.; Lehn, J.-M. *Angew. Chem., Int. Ed.* **2007**, *46*, 6144. (n) Stagni, S.; Orselli, E.; Palazzi, A.; Cola, L. D.; Zacchini, S.; Femoni, C.; Marcaccio, M.; Paolucci, F.; Zanarini, S. *Inorg. Chem.* **2007**, *46*, 9126. (o) Ghumaan, S.; Sarkar, B.; Patil, M. P.; Fiedler, J.; Sunoj, R. B.; Kaim, W.; Lahiri, G. K. *Polyhedron* **2007**, *26*, 3409. (p) Therrien, B.; Süss-Fink, G.; Govindaswamy, P.; Saïd-Mohamed, C. *Polyhedron* **2007**, *26*, 4065. (q) Herrera, J.-M.; Pope, S. J. A.; Meijer, A. J. H. M.; Easun, T. L.; Adams, H.; Alsindi, W. Z.; Sun, X.-Z.; George, M. W.; Faulkner, S.; Ward, M. D. *J. Am. Chem. Soc.* **2007**, *129*, 11491. (r) Xun, S.; Zhang, J.; Li, X.; Ma, D.; Wang, Z. Y. *Synth. Met.* **2008**, *158*, 484. (s) Londergan, C. H.; Salsman, J. C.; Lear, B. J.; Kubiak, C. P. *Chem. Phys.* **2006**, *324*, 57. (t) Salsman, J. C.; Kubiak, C. P.; Ito, T. *J. Am. Chem. Soc.* **2005**, *127*, 2382. (u) Fürholz, U.; Joss, S.; Bürgi, H. B.; Ludi, A. *Inorg. Chem.* **1985**, *24*, 943. (v) Glover, S. D.; Goeltz, J. C.; Lear, B. J.; Kubiak, C. P. *Coord. Chem. Rev.* **2010**, *254*, 331.

(4) (a) Hush, N. S. *Prog. Inorg. Chem.* **1967**, *8*, 391. (b) Hush, N. S. *Coord. Chem. Rev.* **1985**, *64*, 135. (c) Creutz, C.; Newton, M. D.; Sutin, N. *J. Photochem. Photobiol. A* **1994**, *82*, 47.

(5) (a) Petrov, V.; Hupp, J. T.; Mottley, C.; Mann, L. C. *J. Am. Chem. Soc.* **1994**, *116*, 2171. (b) Oh, D. H.; Sano, M.; Boxer, S. G. *J. Am. Chem. Soc.* **1991**, *113*, 6880. (c) Rocha, R. C.; Brown, M. G.; Londergan, C. H.; Salsman, J. C.; Kubiak, C. P.; Shreve, A. P. *J. Phys. Chem. A* **2005**, *109*, 9006.

(6) (a) Prassides, K., Ed.; *Mixed Valency Systems - Applications in Chemistry, Physics and Biology*; Kluwer Academic Publishers: Dordrecht, The Netherlands, 1991. (b) Creutz, C. *Prog. Inorg. Chem.* **1983**, *30*, 1. (c) Richardson, D. E.; Taube, H. *Coord. Chem. Rev.* **1984**, *60*, 107. (d) Crutchley, R. J. *Adv. Inorg. Chem.* **1994**, *41*, 273. (e) Demadis, K. D.; Hartshorn, D. C.; Meyer, T. J. *Chem. Rev.* **2001**, *101*, 2655. (f) Kaim, W.; Sarkar, B. *Coord. Chem. Rev.* **2007**, *251*, 584. (g) Kaim, W.; Lahiri, G. K. *Angew. Chem., Int. Ed.* **2007**, *46*, 1778.

(7) (a) Braun-Sand, S. B.; Wiest, O. *J. Phys. Chem. B* **2003**, *107*, 9624. (b) Braun-Sand, S. B.; Wiest, O. *J. Phys. Chem. A* **2003**, *107*, 285. (c) Wang, Y.; Lieberman, M. *IEEE Trans. Nanotech.* **2004**, *3*, 368. (d) Zhao, P.; Woolard, D.; Seminario, J. M.; Trew, R. *Int. J. High Speed Electronics* **2006**, *16*, 705. (e) Lent, C. S.; Isaksen, B.; Lieberman, M. *J. Am. Chem. Soc.* **2003**, *125*, 1056.

(8) (a) Baumann, J. A.; Meyer, T. J. *Inorg. Chem.* **1980**, *19*, 345. (b) Heyduk, A. F.; Nocera, D. G. *Science* **2001**, *293*, 1639. (c) LeClair, G.; Wang, Z. Y. *J. Solid State Electrochem.* **2009**, *13*, 365.

(9) (a) Callahan, R. W.; Keene, F. R.; Meyer, T. J.; Salmon, D. J. *J. Am. Chem. Soc.* **1977**, *99*, 1064. (b) Nemzek, M. A.; Callahan, R. W. *J. Chem. Soc., Chem. Commun.* **1980**, 1231.

(10) Patra, S.; Sarkar, B.; Maji, S.; Fiedler, J.; Urbanos, F. A.; Jimenez-Aparicio, R.; Kaim, W.; Lahiri, G. K. *Chem.—Eur. J.* **2006**, *12*, 489.

(11) Sedney, D.; Ludi, A. *Inorg. Chim. Acta* **1981**, *47*, 153.

(12) Kar, S.; Sarkar, B.; Ghumaan, S.; Janardan, D.; Slageren, J. V.; Fiedler, J.; Puranik, V. G.; Sunoj, R. B.; Kaim, W.; Lahiri, G. K. *Chem.—Eur. J.* **2005**, *11*, 4901.

(13) Ghumaan, S.; Sarkar, B.; Patra, S.; Parimal, K.; Slageren, J. V.; Fiedler, J.; Kaim, W.; Lahiri, G. K. *Dalton Trans.* **2005**, 706.

(14) (a) Patra, S.; Miller, T. A.; Sarkar, B.; Niemeyer, B. M.; Ward, M. D.; Lahiri, G. K. *Inorg. Chem.* **2003**, *42*, 4707. (b) Kar, S.; Chanda, N.; Mobin, S. M.; Datta, A.; Urbanos, F. A.; Puranik, V. G.; Jimenez-Aparicio, R.; Lahiri, G. K. *Inorg. Chem.* **2004**, *43*, 4911.

(15) (a) Ernst, S.; Kasack, V.; Kaim, W. *Inorg. Chem.* **1988**, *27*, 1146. (b) Kumbhakar, D.; Sarkar, B.; Maji, S.; Mobin, S. M.; Fiedler, J.; Urbanos, F. A.; Jimenez-Aparicio, R.; Kaim, W.; Lahiri, G. K. *J. Am. Chem. Soc.* **2008**, *130*, 17575.

(16) (a) Keene, F. R. *Chem. Soc. Rev.* **1998**, *27*, 185. (b) D'Alessandro, D. M.; Keene, F. R. *Chem. Phys.* **2006**, *324*, 8.

(17) Govindaswamy, P.; Therrien, B.; Süss-Fink, G.; Štďpnička, P.; Ludvík, J. *J. Organomet. Chem.* **2007**, *692*, 1661.

(18) Lau, V. C.; Berben, L. A.; Long, J. R. *J. Am. Chem. Soc.* **2002**, *124*, 9042.

(19) Hartshorn, V.; Daire, N.; Tondreau, V.; Loeb, B.; Meyer, T. J.; White, P. S. *Inorg. Chem.* **1999**, *38*, 3200.
(20) Chanda, N.; Laye, R. H.; Chakraborty, S.; Paul, R. L.; Jeffery, J. C.; Ward, M. D.; Lahiri, G. K. *J. Chem. Soc., Dalton Trans.* **2002**, 3496.
(21) Kundu, T.; Sarkar, B.; Mondal, T. K.; Fiedler, J.; Mobin, S. M.; Kaim, W.; Lahiri, G. K. *Inorg. Chem.* **2010**, *49*, 6565.
(22) Das, A. K.; Sarkar, B.; Fiedler, J.; Záliš, S.; Hartenbach, I.; Strobel, S.; Lahiri, G. K.; Kaim, W. *J. Am. Chem. Soc.* **2009**, *131*, 8895.
(23) Rocha, R. C.; Rein, F. N.; Jude, H.; Shreve, A. P.; Concepcion, J. J.; Meyer, T. J. *Angew. Chem., Int. Ed.* **2008**, *47*, 503.
(24) Das, D.; Das, A. K.; Sarkar, B.; Mondal, T. K.; Mobin, S. M.; Fiedler, J.; Záliš, S.; Urbanos, F. A.; Jiménez-Aparicio, R.; Kaim, W.; Lahiri, G. K. *Inorg. Chem.* **2009**, *48*, 11853.
(25) O'Connor, C. J. *Prog. Inorg. Chem.* **1982**, *29*, 203.
(26) Patra, S.; Sarkar, B.; Mobin, S. M.; Kaim, W.; Lahiri, G. K. *Inorg. Chem.* **2003**, *42*, 6469.
(27) Ghumaan, S.; Sarkar, B.; Patra, S.; Slageren, J. V.; Fiedler, J.; Kaim, W.; Lahiri, G. K. *Inorg. Chem.* **2005**, *44*, 3210.
(28) (a) Koiwa, T.; Masuda, Y.; Shono, J.; Kawamoto, Y.; Hoshino, Y.; Hashimoto, T.; Natarajan, K.; Shimizu, K. *Inorg. Chem.* **2004**, *43*, 6215. (b) Eaton, D. R. *J. Am. Chem. Soc.* **1965**, *87*, 3097. (c) Palmer, R. A.; Fay, R. C.; Piper, T. S. *Inorg. Chem.* **1964**, *3*, 875. (d) Holm, R. H.; Cotton, F. A. *J. Am. Chem. Soc.* **1958**, *80*, 5658. (e) Fay, R. C.; Piper, T. S. *J. Am. Chem. Soc.* **1963**, *85*, 500. (f) Chen, J.-L.; Zhang, X.-U.; Zhang, L.-Y.; Shi, L.-X.; Chen, Z.-N. *Inorg. Chem.* **2005**, *44*, 1037.
(29) Chakraborty, S.; Laye, R. H.; Munshi, P.; Paul, R. L.; Ward, M. D.; Lahiri, G. K. *Dalton Trans.* **2002**, 2348.
(30) Kar, S.; Sarkar, B.; Ghumaan, S.; Roy, D.; Urbanos, F. A.; Fiedler, J.; Sunoj, R. B.; Jimenez-Aparicio, R.; Kaim, W.; Lahiri, G. K. *Inorg. Chem.* **2005**, *44*, 8715.
(31) Ghumaan, S.; Sarkar, B.; Maji, S.; Puranik, V. G.; Fiedler, J.; Urbanos, F. A.; Jimenez-Aparicio, R.; Kaim, W.; Lahiri, G. K. *Chem.—Eur. J.* **2008**, *14*, 10816.
(32) Kaim, W. *Angew. Chem.* **1983**, *95*, 201. *Angew. Chem., Int. Ed.* **1983**, *22*, 171.
(33) Patra, S.; Sarkar, B.; Ghumaan, S.; Fiedler, J.; Kaim, W.; Lahiri, G. K. *Inorg. Chem.* **2004**, *43*, 6108.
(34) (a) Patra, S.; Sarkar, B.; Ghumaan, S.; Patil, M. P.; Mobin, S. M.; Sunoj, R. B.; Kaim, W.; Lahiri, G. K. *Dalton Trans.* **2005**, 1188. (b) Kar, S.; Chanda, N.; Mobin, S. M.; Urbanos, F. A.; Niemeyer, M.; Puranik, V. G.; Jimenez-Aparicio, R.; Lahiri, G. K. *Inorg. Chem.* **2005**, *44*, 1571. (c) Maji, S.; Sarkar, B.; Patra, S.; Fiedler, J.; Mobin, S. M.; Puranik, V. G.; Kaim, W.; Lahiri, G. K. *Inorg. Chem.* **2006**, *45*, 1316.
(35) (a) Stebler, A.; Ammeter, J. H.; Furholz, U.; Ludi, A. *Inorg. Chem.* **1984**, *23*, 2764. (b) Poppe, J.; Moscherosch, M.; Kaim, W. *Inorg. Chem.* **1993**, *32*, 2640.
(36) Kaim, W.; Kasack, V. *Inorg. Chem.* **1990**, *29*, 4696.
(37) Heck, J.; Lange, G.; Malessa, M.; Boese, R.; Bläser, D. *Chem.—Eur. J.* **1999**, *5*, 659.
(38) Maji, S.; Sarkar, B.; Mobin, S. M.; Fiedler, J.; Urbanos, F. A.; Jimenez-Aparicio, R.; Kaim, W.; Lahiri, G. K. *Inorg. Chem.* **2008**, *47*, 5204.
(39) Kober, E. M.; Meyer, T. J. *Inorg. Chem.* **1983**, *22*, 1614.
(40) (a) Cheah, M. H.; Borg, S. J.; Bondin, M. I.; Best, S. P. *Inorg. Chem.* **2004**, *43*, 5635. (b) Kaim, W.; Bruns, W.; Poppe, J.; Kasack, V. *J. Mol. Struct.* **1993**, *292*, 221.
(41) Koley, M.; Sarkar, B.; Ghumaan, S.; Bulak, E.; Fiedler, J.; Kaim, W.; Lahiri, G. K. *Inorg. Chem.* **2007**, *46*, 3736.
(42) Ghumaan, S.; Sarkar, B.; Chanda, N.; Sieger, M.; Fiedler, J.; Kaim, W.; Lahiri, G. K. *Inorg. Chem.* **2006**, *45*, 7955.
(43) Kobayashi, T.; Nishina, Y.; Shimizu, K. G.; Satô, G. P. *Chem. Lett.* **1988**, 1137.
(44) Sawyer, D. T.; Sobkowiak, A.; Roberts, J. L., Jr. *Electrochemistry for Chemists*; Wiley: New York, 1995.
(45) Krejcik, M.; Danek, M.; Hartl, F. *J. Electroanal. Chem.* **1991**, *317*, 179.
(46) Kaim, W.; Ernst, S.; Kasack, V. *J. Am. Chem. Soc.* **1990**, *112*, 173.
(47) Sheldrick, G. M. *SHELX-97, Program for Crystal Structure Solution and Refinement*; University of Göttingen: Göttingen, Germany, 1997.
(48) Lee, C.; Yang, W.; Parr, R. G. *Phys. Rev. B* **1988**, *37*, 785.
(49) (a) Andrae, D.; Haeussermann, U.; Dolg, M.; Stoll, H.; Preuss, H. *Theor. Chim. Acta* **1990**, *77*, 123. (b) Fuentealba, P.; Preuss, H.; Stoll, H.; Szentpaly, L. V. *Chem. Phys. Lett.* **1989**, *89*, 418.
(50) Frisch, M. J.; Trucks, G. W.; Schlegel, H. B.; Scuseria, G. E.; Robb, M. A.; Cheeseman, J. R.; Montgomery, J. A.; Vreven, T. Jr.; Kudin, K. N.; Burant, J. C.; Millam, J. M.; Iyengar, S. S.; Tomasi, J.; Barone, V.; Mennucci, B.; Cossi, M.; Scalmani, G.; Rega, N.; Petersson, G. A.; Nakatsuji, H.; Hada, M.; Ehara, M.; Toyota, K.; Fukuda, R.; Hasegawa, J.; Ishida, M.; Nakajima, T.; Honda, Y.; Kitao, O.; Nakai, H.; Klene, M.; Li, X.; Knox, J. E.; Hratchian, H. P.; Cross, J. B.; Bakken, V.; Adamo, C.; Jaramillo, J.; Gomperts, R.; Stratmann, R. E.; Yazyev, O.; Austin, A. J.; Cammi, R.; Pomelli, C.; Ochterski, J. W.; Ayala, P. Y.; Morokuma, K.; Voth, G. A.; Salvador, P. ; Dannenberg, J. J.; Zakrzewski, V. G. ; Dapprich, S.; Daniels, A. D.; Strain, M. C.; Farkas, O.; Malick, D. K.; Rabuck, A. D.; Raghavachari, K.; Foresman, J. B.; Ortiz, J. V.; Cui, Q.; Baboul, A. G.; Clifford, S.; Cioslowski, J.; Stefanov, B. B.; Liu, G.; Liashenko, A.; Piskorz, P.; Komaromi, I.; Martin, R. L.; Fox, D. J.; Keith, T.; Al-Laham, M. A.; Peng, C. Y.; Nanayakkara, A.; Challacombe, M.; Gill, P. M. W.; Johnson, B.; Chen, W.; Wong, M. W.; Gonzalez, C.; Pople, J. A. *Gaussian 03*; Gaussian, Inc.: Wallingford, CT, 2004.
(51) (a) Bauernschmitt, R.; Ahlrichs, R. *Chem. Phys. Lett.* **1996**, *256*, 454. (b) Stratmann, R. E.; Scuseria, G. E.; Frisch, M. J. *J. Chem. Phys.* **1998**, *109*, 8218. (c) Casida, M. E.; Jamorski, C.; Casida, K. C.; Salahub, D. R. *J. Chem. Phys.* **1998**, *108*, 4439.
(52) (a) Barone, V.; Cossi, M. *J. Phys. Chem. A* **1998**, *102*, 1995. (b) Cossi, M.; Barone, V. *J. Chem. Phys.* **2001**, *115*, 4708. (c) Cossi, M.; Rega, N.; Scalmani, G.; Barone, V. *J. Comput. Chem.* **2003**, *24*, 669.
(53) O'Boyle, N. M.; Tenderholt, A. L.; Langner, K. M. *J. Comput. Chem.* **2008**, *29*, 839.